positive if the negative signal area on 3D-real IR in the vestibule is more than a quarter of the entire vestibule. These tentative criteria were established based on previous histological research in humans and animals [13–15].

Results

In all patients, low signal of endolymphatic space in the labyrinth on 3D-FLAIR was observed in the anatomically appropriate position, and it showed negative signal on 3D-real IR. The low signal area of surrounding bone on 3D-FLAIR showed near zero signal on 3D-real IR (Figs. 1, 2, 3). Gd-containing perilymphatic space showed high signal on 3D-real IR images. The spatial relationship between endolymphatic space and perilymphatic space can be well appreciated on 3D-real IR images. In nine Meniere's disease patients and two patients with acute low-tone sensorineural hearing loss, the endolymphatic space was enlarged. In the two patients with acute low-tone sensorineural hearing loss, endolymphatic space in the upper turn of the cochlea seemed to be more enlarged, while perilymphatic space of the scala vestibuli seemed to be narrower compared to that of the lower turn. In two cases of delayed endolymphatic hydrops, both the left and right ears showed endolymphatic hydrops.

No side effect relating to intratympanic administration of Gd-DTPA was observed.

Discussion

Separate visualization of perilymph and endolymph fluid space by MR imaging has been tried by several researchers [16]. Direct visualization of Reissner's membrane using high spatial resolution imaging was successful in animals [17] and human cadavers [18, 19]; however, clear visualization in living human subjects has not been successful due to the limited spatial resolution of clinical MR imaging units [20, 21].

Intravenous administration of Gd-DTPA in healthy human volunteers resulted in a slight signal increase in the labyrinth after 4 h [22]. However, the separation between the endolymphatic space and perilymphatic space was not clear, probably due to an insufficient concentration of Gd in the perilymphatic space.

Intratympanic injection of Gd-DTPA and the utilization of 3D FLAIR at 3 T made the visualization of endolymphatic hydrops possible in vivo [2]. Intratympanically administered Gd-DTPA distributed mainly into perilymphatic fluid space, and not into endolymphatic space. However, it was difficult to differentiate the low signal of endolymphatic space on 3D FLAIR from surrounding bone. Especially endolymphatic space in the vestibule is difficult to delineate when it is enlarged [2].

To delineate endolymphatic space precisely and to allow the quantification of endolymphatic-space volume in the future, endolymphatic space needs to be visualized separately, not only from perilymphatic space, but also from bone and air. By changing the inversion time, endolymphatic space and perilymphatic space might be separately visualized as positive signal. This will allow the volume quantification of each space in the future.

Quantification of each space is an important goal in the future for the objective diagnosis of endolymphatic hydrops and for monitoring treatment efficacy. Even with current spatial resolution however, it will take 30 min to

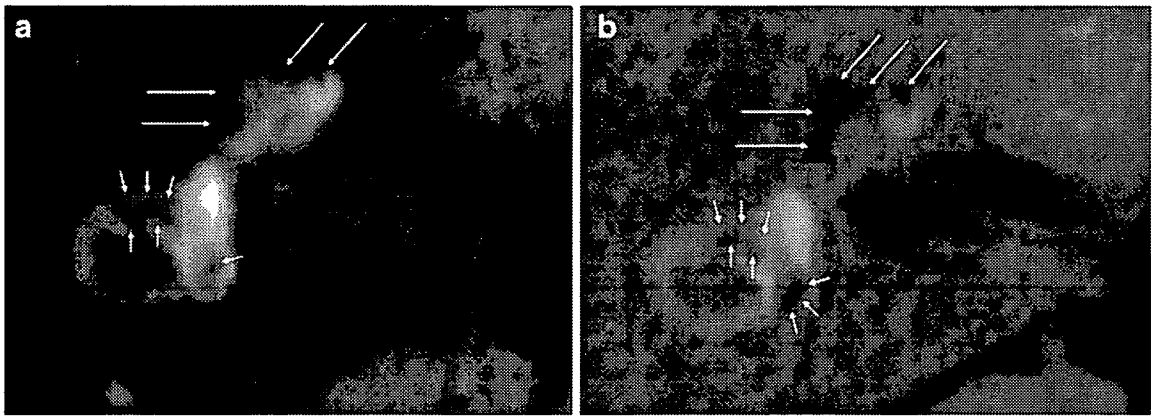

Fig. 1 A 31-year-old man with acute low-tone senrorineural hearing loss in the right ear (average, 31 dB). All images were obtained 24 h after the intratympanic injection of Gd-DTPA. (**a**) 3D-FLAIR (9,000/134/2,500) shows enlarged endolymphatic space in the cochlea (arrows) as low signal areas; however, the boundary between endolymphatic space and surrounding bone is unclear. Mild enlargement of the endolymphatic space in the vestibule (short arrows) is observed. (**b**) A 3D-real IR sequence (9,000/134/1,700) visualizes severely enlarged endolymphatic space in the cochlea (arrows) and mildly enlarged endolymphatic space in the vestibule (short arrows) as negative signal intensity values, while the surrounding bone area has near zero signal intensity. This image allows the separation of perilymph space (high signal intensity), endolymph space and surronding bone on a single image. In this acute low-tone senrorineural hearing loss patient, perilymphatic space in the upper cochlear turn seems to be narrower than in the lower turn due to relatively severe endolymphatic hydrops in the upper turn

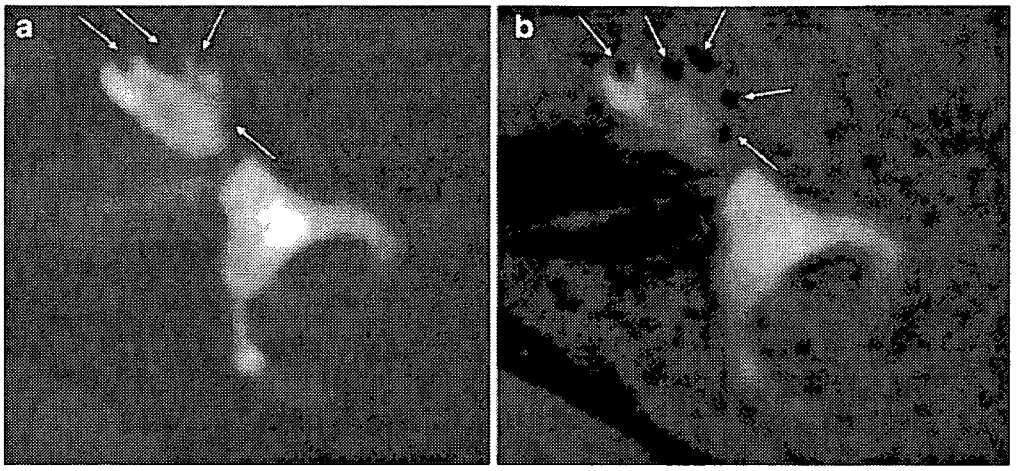

Fig. 2 A 33-year-old man with delayed endolymphatic hydrops. All images were obtained 24 h after the intratympanic injection of Gd-DTPA. (**a**) 3D-FLAIR (9,000/134/2,500) shows enlarged endolymphatic space in the cochlea (arrows), but not in the vestible. The boundary between endolymphatic space and surrounding bone is unclear. (**b**) A 3D-real IR sequence (9,000/134/1,700) visualizes severely enlarged endolymphatic space in all cochlear turns (arrows) as negative signal intensity values, while the surrounding bone area has near zero signal intensity. This image makes possible the delineation of the scala media (negative signal intensity; black on this image) from perilymph space (scala tympani and scala vestibuli with positive high signal intensity; white on this image) and surronding bone (near zero signal; gray on this image) on a single image

obtain both endolymphatic images and perilymphatic images separately. Furthermore, the spatial relationship between the two spaces cannot be appreciated without the fusion of two separately obtained images. Non-uniform distribution of Gd-DTPA in the perilymphatic space also would make it difficult to uniformly suppress the signal of perilymphatic fluid with a single inversion time.

The present method with 3D inversion recovery using real reconstruction divides the signal magnitude of the endo- and perilymphatic fluid into positive and negative; thus, the precise value of the inversion time is not as important.

One of the limitations of the present method is the relatively low spatial resolution in the slice direction due to limited scan time and signal-to-noise ratio. To improve the signal-to-noise ratio, further study is necessary to investigate strategies that reduce acquisition time (and improve imaging efficiency), such as shorter TR and longer echo-train length. A shorter acquisition time would allow us to obtain higher spatial resolution or a larger number of excitations.

Another limitation of this study is the lack of histological confirmation for the presence of endolymphatic hydrops. It is virtually impossible to obtain histological proof in human

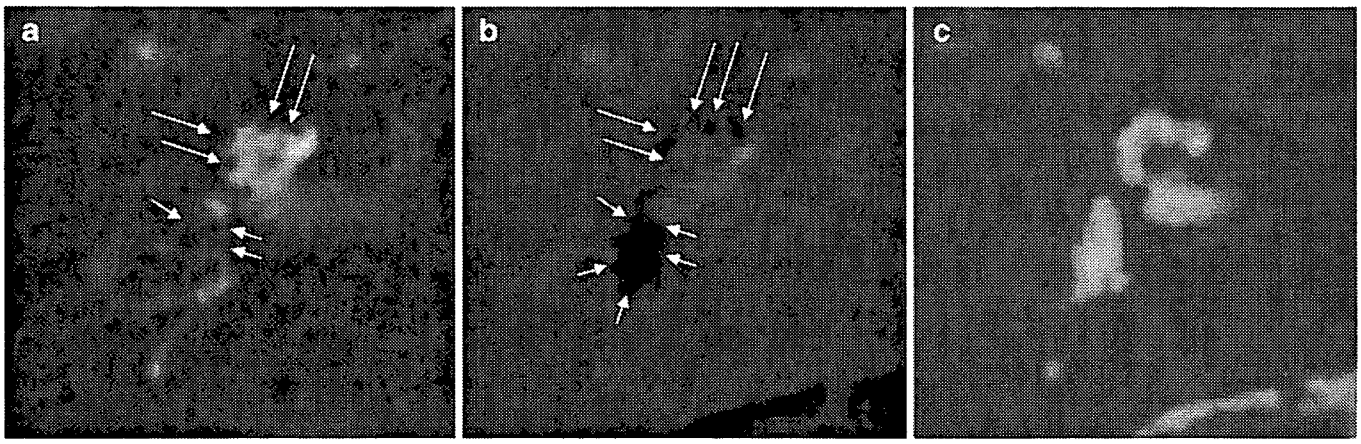

Fig. 3 A 42-year-old man with Meniere's disease. All images were obtained 24 h after the intratympanic injection of Gd-DTPA. (**a**) 3D-FLAIR (9,000/134/2,500) shows severely enlarged endolymphatic space in the cochlea (arrows) and in the vestibule (short arrows). The boundary between endolymphatic space and surrounding bone is unclear. (**b**) A 3D-real IR sequence (9,000/134/1,700) visualizes severely enlarged endolymphatic space in all cochlear turns (arrows) and in the vestibule (short arrows) as negative signal intensity values, while the surrounding bone area has near zero signal intensity. (**c**) 3D-CISS (11.42/5.71/flip angle 50 degree) image shows the combination of endolymphatic and perilymphatic space

patients; therefore, animal experiments would be important to validate the results of this study. Clinical diagnosis of endolymphatic hydrops is based on patients' history, symptoms and various otological tests. However, proof of endolymphatic hydrops in a particular patient is rarely obtained. Besides the animal experiments, the accumulation of follow-up MR-imaging studies using present methods, showing a correlation between the progression of image findings and clinical records, would be necessary to verify the utility of the present method using a 3D inversion-recovery sequence with real reconstruction.

Some invasiveness and relatively long scan time might prevent the wide spread of this method in the clinical setting, especially in the period of acute vertigo attack of Meniere's disease. Rupture of Reissner's membrane during the attack might cause the contamination of endo- and perilymph fluid, and severely decrease the significance of this method.

In conclusion, by optimizing the inversion time, endolymphatic space, perilymphatic space and surrounding bone or air can be separately visualized on a single image using a 3D inversion-recovery sequence with real reconstruction. This method might open the door for the objective evaluation of endolymphatic space disease in clinical settings.

References

1. Zou J, Pyykko I, Bjelke B, Dastidar P, Toppila E (2005) Communication between the perilymphatic scalae and spiral ligament visualized by in vivo MRI. Audiol Neurootol 10(3):145–152
2. Nakashima T, Naganawa S, Sugiura M, Teranishi M, Sone M, Hayashi H, Nakata S, Katayama N, Ishida IM (2007) Visualization of endolymphatic hydrops in patients with Meniere's disease. Laryngoscope 117(3):415–420
3. Park HW, Cho MH, Cho ZH (1986) Real-value representation in inversion-recovery NMR imaging by use of a phase-correction method. Magn Reson Med 3(1):15–23
4. Bandai H, Tsunoda A, Mitsuoka H, Arai H, Sato K, Makita J (2002) Fast inversion recovery magnetic resonance imaging with the real reconstruction method: a diagnostic tool for cerebral gliomas. Neurol Med Chir (Tokyo) 42 (1):5–10
5. Naganawa S, Koshikawa T, Nakamura T, Fukatsu H, Ishigaki T, Aoki I (2003) High-resolution T1-weighted 3D real IR imaging of the temporal bone using triple-dose contrast material. Eur Radiol 13(12):2650–2658
6. Schuknecht HF, Suzuka Y, Zimmermann C (1990) Delayed endolymphatic hydrops and its relationship to Meniere's disease. Ann Otol Rhinol Laryngol 99(11):843–853
7. Fujino K, Naito Y, Endo T, Kanemaru S, Hiraumi H, Tsuji J, Ito J (2007) Clinical characteristics of delayed endolymphatic hydrops: long-term results of hearing and efficacy of hyperbaric oxygenation therapy. Acta Otolaryngol Suppl 1557:22–25
8. Schwaber MK (2002) Transtympanic gentamicin perfusion for the treatment of Meniere's disease. Otolaryngol Clin North Am 35(2):287–295
9. Haynes DS, O'Malley M, Cohen S, Watford K, Labadie RF (2007) Intratympanic dexamethasone for sudden sensorineural hearing loss after failure of systemic therapy. Laryngoscope 117(1):3–15
10. Ahn JH, Han MW, Kim JH, Chung JW, Yoon TH (2007) Therapeutic effectiveness over time of intratympanic dexamethasone as salvage treatment of sudden deafness. Acta Otolaryngol. 2007 Aug 22; 1-4 [Epub ahead of print] DOI 10.1080/00016480701477602
11. De Stefano A, Dispenza F, De Donato G, Caruso A, Taibah A, Sanna M (2007) Intratympanic gentamicin: a 1-day protocol treatment for unilateral Meniere's disease. Am J Otolaryngol 28(5):289–293
12. Griswold MA, Jakob PM, Heidemann RM, Nittka M, Jellus V, Wang J, Kiefer B, Haase A (2002) Generalized autocalibrating partially parallel acquisitions (GRAPPA). Magn Reson Med 47 (6):1202–1210
13. Salt AN, Henson MM, Gewalt SL, Keating AW, DeMott JE, Henson OW, Jr (1995) Detection and quantification of endolymphatic hydrops in the guinea pig cochlea by magnetic resonance microscopy. Hear Res 88(1-2):79–86
14. Shinomori Y, Spack DS, Jones DD, Kimura RS (2001) Volumetric and dimensional analysis of the guinea pig inner ear. Ann Otol Rhinol Laryngol 110(1):91–98
15. Buckingham RA, Valvassori GE (2001) Inner ear fluid volumes and the resolving power of magnetic resonance imaging: can it differentiate endolymphatic structures? Ann Otol Rhinol Laryngol 110(2):113–117
16. Niyazov DM, Andrews JC, Strelioff D, Sinha S, Lufkin R (2001) Diagnosis of endolymphatic hydrops in vivo with magnetic resonance imaging. Otol Neurotol 22(6):813–817
17. Koizuka I, Seo Y, Murakami M, Seo R, Kato I (1997) Micro-magnetic resonance imaging of the inner ear in the guinea pig. NMR Biomed 10(1):31–34
18. Koizuka I, Seo R, Kubo T, Matsunaga T, Murakami M, Seo Y, Watari H (1995) High-resolution MRI of the human cochlea. Acta Otolaryngol Suppl 520(Pt 2):256–257
19. Koizuka I, Seo R, Sano M, Matsunaga T, Murakami M, Seo Y, Watari H (1991) High-resolution magnetic resonance imaging of the human temporal bone. ORL J Otorhinolaryngol Relat Spec 53(6):357–361
20. Ito T, Naganawa S, Fukatsu H, Ishiguchi T, Ishigaki T, Kobayashi M, Kobayashi K, Ichinose N, Miyazaki M, Kassai Y (1999) High-resolution MR images of inner ear internal anatomy using a local gradient coil at 1.5 Tesla: correlation with histological specimen. Radiat Med 17(5):343–347
21. Naganawa S, Koshikawa T, Fukatsu H, Ishigaki T, Aoki I, Ninomiya A (2002) Fast recovery 3D fast spin-echo MR imaging of the inner ear at 3 T. AJNR Am J Neuroradiol 23(2):299–302
22. Naganawa S, Komada T, Fukatsu H, Ishigaki T, Takizawa O (2006) Observation of contrast enhancement in the cochlear fluid space of healthy subjects using a 3D-FLAIR sequence at 3 Tesla. Eur Radiol 16(3):733–737